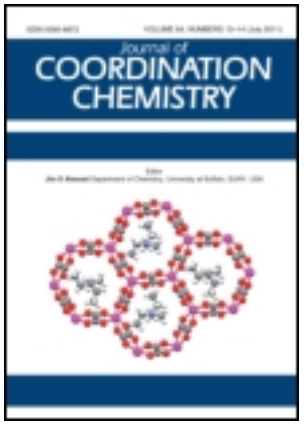

Journal of Coordination Chemistry
Publication details, including instructions for authors and subscription information:
http://www.tandfonline.com/loi/gcoo20

Mixed-ligand manganese(II)-phenolate complexes: study of DNA cleavage, cytotoxic activity, and induction of apoptosis

En-Jun Gao [a], Ying Zhang [a], Lin Lin [a], Ren-Shu Wang [a], Lei Dai [a], Qi Liang [a], Ming-Chang Zhu [a], Mei-Lin Wang [a], Lei Liu [a], Wen-Xuan He [a] & Yan-Jin Zhang [a]

[a] Department of Coordination Chemistry, International Key Laboratory of Shenyang Inorganic Molecule-Based Chemical, Shenyang University of Chemical Technology, Shenyang 110142, China

Version of record first published: 11 Nov 2011

To cite this article: En-Jun Gao, Ying Zhang, Lin Lin, Ren-Shu Wang, Lei Dai, Qi Liang, Ming-Chang Zhu, Mei-Lin Wang, Lei Liu, Wen-Xuan He & Yan-Jin Zhang (2011): Mixed-ligand manganese(II)-phenolate complexes: study of DNA cleavage, cytotoxic activity, and induction of apoptosis, Journal of Coordination Chemistry, 64:22, 3992-4005

To link to this article: http://dx.doi.org/10.1080/00958972.2011.634910

Journal of Coordination Chemistry
Vol. 64, No. 22, 20 November 2011, 3992–4005

Mixed-ligand manganese(II)-phenolate complexes: study of DNA cleavage, cytotoxic activity, and induction of apoptosis

EN-JUN GAO*, YING ZHANG, LIN LIN, REN-SHU WANG, LEI DAI, QI LIANG, MING-CHANG ZHU, MEI-LIN WANG, LEI LIU, WEN-XUAN HE and YAN-JIN ZHANG

Department of Coordination Chemistry, International Key Laboratory of Shenyang Inorganic Molecule-Based Chemical, Shenyang University of Chemical Technology, Shenyang 110142, China

(*Received 21 August 2011; in final form 14 October 2011*)

Two manganese complexes, $[Mn(L^1)_2(dibe)_2](L^1)$ (**1**) and $[Mn(L^2)_2(dibe)_2]$ (**2**) (where $L^1 = 2,2'$-bipyridine (bipy), $L^2 = 1,10$-phenanthroline (phen)), were synthesized by using a carboxylic acid ligand (dibe = 2,2-dibenzylmalonate acid). The two complexes were characterized using IR, elemental analysis, and X-ray crystallography. Fluorescence analysis indicates that the two complexes can bind to HeLa cell DNA (HC-DNA), and gel electrophoresis assay demonstrates the ability of the complexes to cleave the HC-DNA. The two complexes exhibit cytotoxic specificity and significant cancer cell inhibitory rate. Furthermore, apoptotic tests demonstrate that these two complexes have apoptotic effects on HeLa cells.

Keywords: Manganese; Fluorescence; Cleavage; Cytotoxicity; Apoptosis

1. Introduction

There has been substantial interest in the design and investigation of transition-metal anticancer drugs [1–4]. Metal-based anticancer drugs, e.g. cisplatin, are widely used in clinics. However, severe side effects occur after treatment [5–10]. Accordingly, it is indispensable to develop less toxic, more-efficacious and target-specific metal-based anticancer drugs in pharmaceutical research. Numerous transition-metal complexes are synthesized and screened for their anticancer activities.

The design of these metal-based pharmaceuticals depends on the ligand framework, the metal ion, and its oxidation state. Ligands can significantly alter the biological activities of complex. Tailored, multifunctional ligands introduced into metal-based medicinal agents limit the adverse effects of metal ion [11–13]. Carboxylic acids are widely used as ligands as they can easily coordinate with metal by protonation [14]. Research on complexes with 1,10-phenanthroline (phen) and bipyridine (bipy) show that the complexes have strong intercalation with DNA, high DNA cleavage efficiency and cytotoxicity [15, 16]. We have reported palladium(II), platinum(II), copper(II),

*Corresponding author. Email: ejgao@yahoo.com.cn

ISSN 0095-8972 print/ISSN 1029-0389 online © 2011 Taylor & Francis
http://dx.doi.org/10.1080/00958972.2011.634910

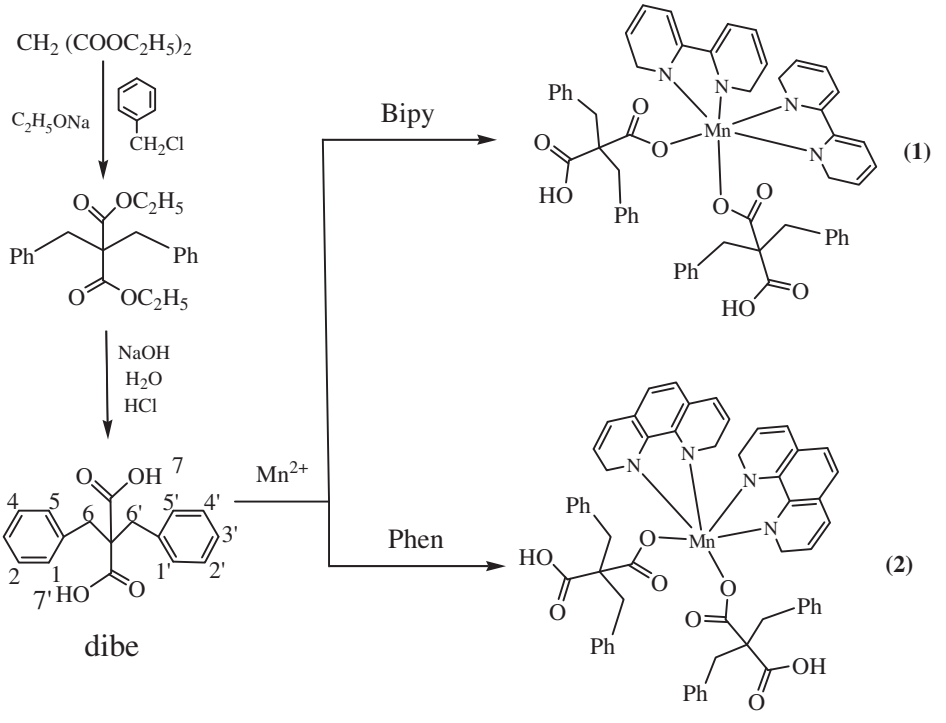

Scheme 1. Schematic structure of the two complexes and the numbering scheme for ^{1}H NMR spectroscopy.

cobalt(II), and zinc(II) complexes with prominent anticancer activities [17–25]. As an important transition-metal element, manganese can also form complexes and some manganese complexes exhibit excellent biological activities [26, 27].

In the present work, two Mn(II) complexes, $[Mn(L^1)_2(dibe)_2](L^1)$ (**1**) and $[Mn(L^2)_2(dibe)_2]$ (**2**), were synthesized and characterized (dibe is 2,2-dibenzylmalonate acid synthesized in our laboratory, shown in scheme 1). L^1 and L^2 are bipy and phen, respectively. The DNA-cleaving and Hela cell apoptosis of the complexes have been investigated by gel electrophoresis and MTT assay, respectively. The cytotoxic effects of these complexes were examined on four cancer cell lines, HeLa, Hep-G2, KB, and AGZY-83a.

2. Experimental

2.1. *Materials*

Chemicals purchased were of reagent-grade and used without purification unless otherwise noted. All spectroscopic titration was carried out in aerated buffer (5 mmol L^{-1} Tris-HCl, 50 mmol L^{-1} NaCl, pH = 7.2) at room temperature. HC-DNA applied here was extracted by us. The HeLa (human cervix epitheloid carcinoma) cells, the Hep-G2 (human hepatocellular carcinoma) cells, the KB (human oral epithelial

carcinoma) cells and the AGZY-83a (human lung carcinoma) cells were obtained from American Type Culture Collection.

2.2. *Ligand synthesis*

A total of 80 mL of sodium ethoxide and 30 mL of diethyl malonate were mixed, stirred and heated to 80°C for 6 min, then 50 mL of benzyl chloride was dropwise added to the mixture. The mixture was refluxed for 15 min, allowed to cool and washed with deionized water. The organic phase was removed and the residue was extracted with ethyl acetate which was distilled off and the fraction was acquired by vacuum distillation. After dropwise adding the fraction to sodium hydroxide and cooling it to room temperature, white crude solid appeared. Dissolving it to deionized water, heating and acidifying its pH close to $1 \sim 2$, white solid 2,2-dibenzylmalonic acid appeared after distilling. Yield: 34%. This step of reaction is shown in scheme 1. IR (cm^{-1}, s, strong; m, medium): ν(–O–H) 3417(m), ν(=C–H) 3028(m), ν(–C=O) 1715(s), ν(C=C) 1591(s). ^{1}H NMR (DMSO-d_6, 300 MHz): δ 9.27 (s, 2H, H7, H7′), 7.40 (t, $J = 8.1$ Hz, 4H, H2, H2′, H4, H4′), 7.29 (d, $J = 7.5$ Hz, 4H, H1, H1′, H5, H5′), 7.27 (t, $J = 7.8$ Hz, 2H, H3, H3′), 3.13(s, 2H, H6, H6′).

2.3. *Complex synthesis*

2.3.1. Synthesis of $C_{64}H_{54}Mn_1N_6O_8$. Complex **1** was prepared as follows: dibe was dissolved in a KOH aqueous solution. Then a $Mn(CH_3COO)_2$ aqueous solution (10 mmol, 10 mL) and an aqueous solution of L (10 mmol, 10 mL) were mixed, and the pH adjusted to acidity, and the mixture stirred at room temperature. After reacting for 4 h, bipy ethanolic solution (10 mmol, 10 mL) was added and the mixture appeared turbid; continuing stirring for 2 h, the clear solution was obtained after filtration under atmospheric pressure. Several days later, golden yellow transparent crystals formed by evaporating the solution at room temperature, were collected and found suitable for X-ray crystallography. The crystals were collected by filtration. For $C_{64}H_{54}Mn_1N_6O_8$, Anal. Calcd (%): C, 70.52; H, 4.99; N, 7.71. Found (%): C, 70.49; H, 5.07; N, 7.64. IR (cm^{-1}, s, strong; m, medium): ν(–O–H) 3417(m); ν(COO^-) 1678(s); ν(C=C) 1578(s); ν(C–N) 1440(s); δ(–C–H) 1610(m).

2.3.2. Synthesis of $C_{58}H_{46}Mn_1N_4O_8$. Complex **2** was synthesized in an identical manner as described for **1** with phen (10 mmol 10 mL) in place of bipy (shown in scheme 1). The product was obtained as brown powder. Yield: 69%. For $C_{58}H_{46}Mn_1N_4O_8$, Anal. Calcd (%): C, 70.94; H, 4.22; N, 5.71. Found (%): C, 70.90; H, 4.31; N, 5.69. IR (cm^{-1}, s, strong; m, medium): ν(–O–H) 3385(m); ν(COO^-) 1610(s); ν(C=C) 1575(s); ν(–C–N) 1328(s); δ(–C–H) 1609(m).

2.4. *Physical measurements*

Elemental analysis (C, H, and N) was performed on a model Finnigan EA 1112. IR spectra were obtained as KBr pellets on a Nicolet FT-IR 470 spectrometer.

2.5. *X-ray crystallographic determination for 1*

Data of **1** were collected on a Bruker Smart 1000 CCD X-ray single-crystal diffractometer with Mo-Kα radiation ($\lambda = 0.71073$ Å) at 293(2) K, and intensity data were obtained from $1.71^\circ \leq \theta \leq 25.68^\circ$ at 293(2) K by using an ω scan technique. Corrections for the *Lp* factor and an empirical absorption correction were applied. The structure was solved by direct methods using SHELXS-97. All non-hydrogen atoms were determined with successive difference Fourier syntheses and refined by full matrix least squares on F^2. All hydrogen atoms were located at theoretical positions. CCDC reference number is 807131.

2.6. *Cell line and culture*

The cell lines used in this experiment were routinely maintained in a RPMI-1640 medium supplemented with 10% (v/v) heat inactivated fetal bovine serum, 2 mmol L^{-1} of glutamine, 100 u mL^{-1} of penicillin, and 100 µg mL^{-1} of streptomycin in a highly humidified atmosphere of 95% air with 5% CO_2 at 37°C.

2.7. *Extraction of HC-DNA*

HeLa cells were grown adherently on the culture flask at 37°C under sterile conditions after 2–3 days of growth for extraction. According to our previous work [25], saturated sodium chloride extraction method was used to extract DNA.

2.8. *Fluorescence spectroscopic studies*

Evidence for the two complexes binding to HC-DNA *via* intercalation is given through emission quenching experiment. The experiments of HC-DNA competitive binding with ethidium bromide were carried out in buffer by keeping [DNA]/[EtBr] = 2.5 ([DNA] = 2.5 µmol L^{-1}, [EtBr] = 1 µmol L^{-1}) and varying the concentrations of the metal complexes (0–17 µmol L^{-1}). The buffer used in the binding studies was 50 mmol L^{-1} Tris-HCl, pH = 7.4, containing 10 mmol L^{-1} NaCl. The sample was incubated 4 h at room temperature (20°C) before spectral measurements. For all fluorescence measurements, both the entrance and exit slits were maintained at 10 nm. The excitation wavelength was 526 nm and the emission range was set between 550 and 750 nm.

2.9. *Gel electrophoresis experiments*

The HC-DNA was kept at −20°C. The sample was incubated at 310 K for an appropriate time and a loading buffer was applied (0.25% bromphenol blue, 50% glycerol). For gel electrophoresis experiments, HC-DNA (0.5 mg mL^{-1}) was treated with the complexes. After incubation, the solution was subjected to electrophoresis on 0.8% agarose gel in a TAE buffer (40 mmol L^{-1} Tris acetate 1 mm^{-1} EDTA) at 120 V for 1 h. After electrophoresis, the gel was stained with 1.0 mg mL^{-1} EB and photographed under UV light.

2.10. *Cytotoxicity assay*

The growth inhibitory effect of metal complexes on HeLa cells was measured using the microculture tetrazolium [3-(4,5-dimethylthiazol-2-yl)-2,5-diphenyltetrazoliumbromide, MTT] assay. In brief, cells were seeded into a 96-well culture plate at 2×10^5 cells/well in a 100 μL culture medium. After incubation for 24 h, cells were exposed to the tested complexes of serial concentrations. The complexes were dissolved in DMF and diluted with RPMI 1640 or DMEM to the required concentrations prior to use (0.1% DMF final concentration). The cells were incubated for 24 h and 72 h, followed by addition of a 20 μL MTT solution (5 mg mL^{-1}) to each well and further cultivation for 4 h. The media with MTT were removed and 100 μL of DMSO was added to dissolve the formazan crystals at room temperature for 30 min. The absorbance of each cell at 450 nm was determined by analysis with a micro plate spectrophotometer. The IC_{50} values were obtained from the results of quadruplicate determinations of at least three independent experiments.

In another experiment, the effects on cell growth for the two complexes and cisplatin were studied by culturing the cells in medium alone for 24 h, followed by 72 h treatment with 3 mg mL^{-1} concentration. The viable cells remaining at the end of the treatment period were determined by MTT assay and calculated as the percent of control, treated with the vehicle alone (DMSO) under similar conditions.

2.11. In vitro *apoptotic assay*

HeLa cells in usable condition were seeded in a 24-well culture plate at 2×10^5 cells/well in a 1 mL culture medium, and 24 h later the medium including the cisplatin was given. The concentration of the two complexes was 1 μmol L^{-1} mL^{-1}. The level of apoptosis was evaluated in at least three independent experiments. The hematoxyline–eosin stain was the means of the apoptotic morphology observed by light microscopy. Under the light microscope, the cytoplasm had been stained pink with blue-black in the nucleolus.

3. Results and discussion

3.1. *Crystallographic structure of 1*

The crystal structure of **1** was determined by X-ray crystallography (figure 1). Complex **1** belongs to the monoclinic system with space group *P2(1)/c*. A summary of data collection and refinement for the complex is presented in table 1, and selected bond distances and angles are given in table 2. As shown in figure 2, Mn is six coordinate with two bipy molecules and two oxygens from two carboxyls of dibe; manganese forms an approximate octahedral geometry. The main bond lengths are: Mn–O(1) 2.1023(13) Å, Mn–O(8) 2.1203(14) Å, Mn–N(1) 2.3016(16) Å, Mn–N(2) 2.2535(16) Å, Mn–N(3) 2.3193(16) Å, Mn–N(4) 2.2527(16) Å. In the equatorial plane, the sum of their bond angles [O1–Mn–N4 = 92.04(6), O1–Mn–N2 = 102.04(6), N4–Mn–N1 = 92.56(6), N2–Mn–N1 = 72.46(6)] is 359.10°, close to 360°. In the axial direction, apical N3–Mn–O8 bond angle is 173.99(6)°, close to 180°. Bond lengths among all Mn–O are less than the bond lengths with all Mn–N, suggesting coordination of oxygen from

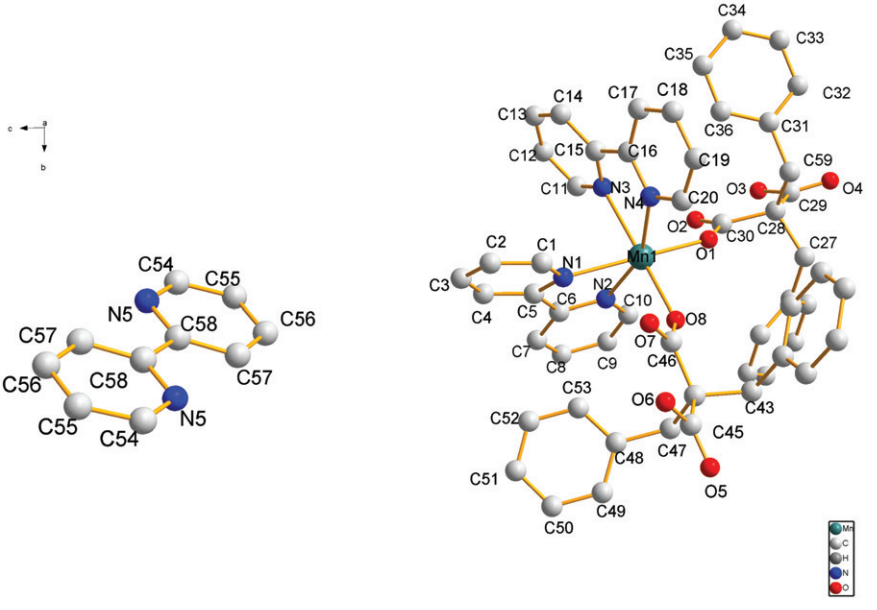

Figure 1. Complex **1** with numbering scheme (H atoms were omitted for clarity) at 30% probability thermal ellipsoids.

Table 1. Crystal data and refinement for **1**.

Parameter	Value
Formula weight	1090.11
Crystal system	Monoclinic
Space group	*P2(1)/c*
Unit cell dimensions (Å, °)	
a	16.4351(10)
b	14.3731(9)
c	22.0276(13)
α	90.00(0)
β	103.2000(10)
γ	90.00(0)
Volume (Å^3), *Z*	5066.0(5), 4
ρ_{Calcd} (g cm^{-3})	1.327
μ_{Mo} (mm^{-1})	0.323
Crystal size (mm^3)	$0.14 \times 0.21 \times 0.19$
θ range for data collection (°)	$1.24 < \theta < 26.23$
Limiting indices	$-19 \le h \le 19$; $-15 \le k \le 17$; $-26 \le l \le 23$
F(000)	2112.0
Reflections collected/unique [$I > 2\sigma(I)$]	27,925/9556 [R(int) = 0.0346]
Completeness (%)	99.3
Number of refined parameters	660
Goodness-of-fit on F^2	1.017
Final R indices [$I > 2\sigma(I)$]	$R_1 = 0.0400$, $wR_2 = 0.0887$
R indices (all data)	$R_1 = 0.0619$, $wR_2 = 0.0980$
$\Delta\rho$ (max) and $\Delta\rho$ (min) (e Å^{-3})	0.33 and −0.213

Table 2. Selected bond lengths (Å) and angles (°) for **1**.

Mn(1)–O(1)	2.1023(14)	Mn(1)–N(2)	2.2535(16)
Mn(1)–O(8)	2.1203(13)	Mn(1)–N(1)	2.3016(16)
Mn(1)–N(4)	2.2527(16)	Mn(1)–N(3)	2.3193(16)
O(1)–Mn(1)–O(8)	88.40(5)	N(4)–Mn(1)–N(1)	92.56(6)
O(1)–Mn(1)–N(4)	92.04(6)	N(2)–Mn(1)–N(1)	72.46(6)
O(8)–Mn(1)–N(4)	102.91(6)	O(1)–Mn(1)–N(3)	94.88(6)
O(1)–Mn(1)–N(2)	102.02(6)	O(8)–Mn(1)–N(3)	173.99(6)
O(8)–Mn(1)–N(2)	94.96(6)	N(4)–Mn(1)–N(3)	71.98(6)
N(4)–Mn(1)–N(2)	157.57(6)	N(2)–Mn(1)–N(3)	89.30(6)
O(1)–Mn(1)–N(1)	174.03(6)	N(1)–Mn(1)–N(3)	82.93(6)
O(8)–Mn(1)–N(1)	94.28(6)		

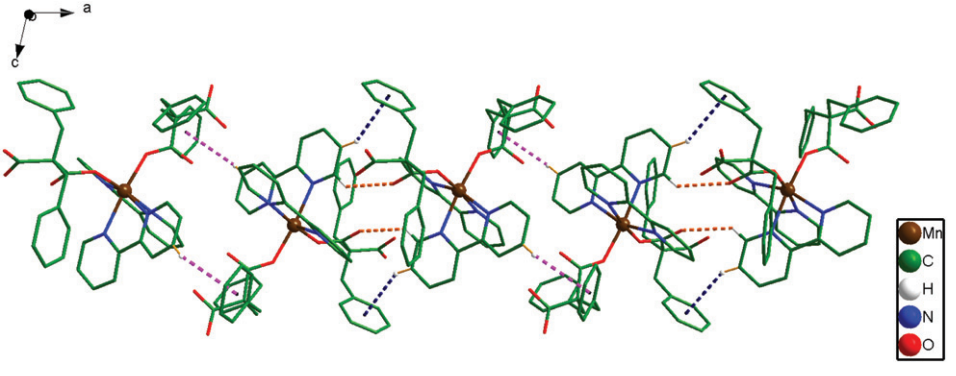

Figure 2. 1-D chain structure of **1**, C–H $\cdots\pi$ and C–H $\cdots$ O interactions (shown by dotted lines).

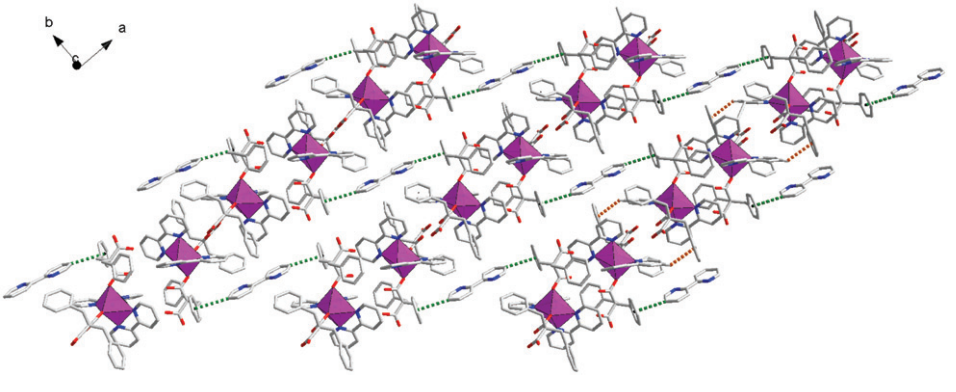

Figure 3. 2-D framework diagram of **1** and the C–H $\cdots\pi$ interactions (shown by dotted lines).

dibe is stronger than nitrogen from bipy. The bond lengths mentioned above are in accord with bond lengths of Mn–N and Mn–O in other coordination compounds [28]. Two adjacent asymmetric complexes form a basic repeat unit *via* C–H $\cdots\pi$ (2.9205 Å) and C–H $\cdots$ O (2.6468 Å) interactions [29–31]. The basic units connect to form a 1-D structure. The 1-D structure forms an undulated layer 2-D structure by C–H $\cdots\pi$ interactions (2.5094 Å) with the dissociated bipy (shown in figure 3) [32]. The 2-D layers further form a 3-D framework *via* weak edge $\pi\cdots\pi$ stacking interactions (3.556 Å) [33].

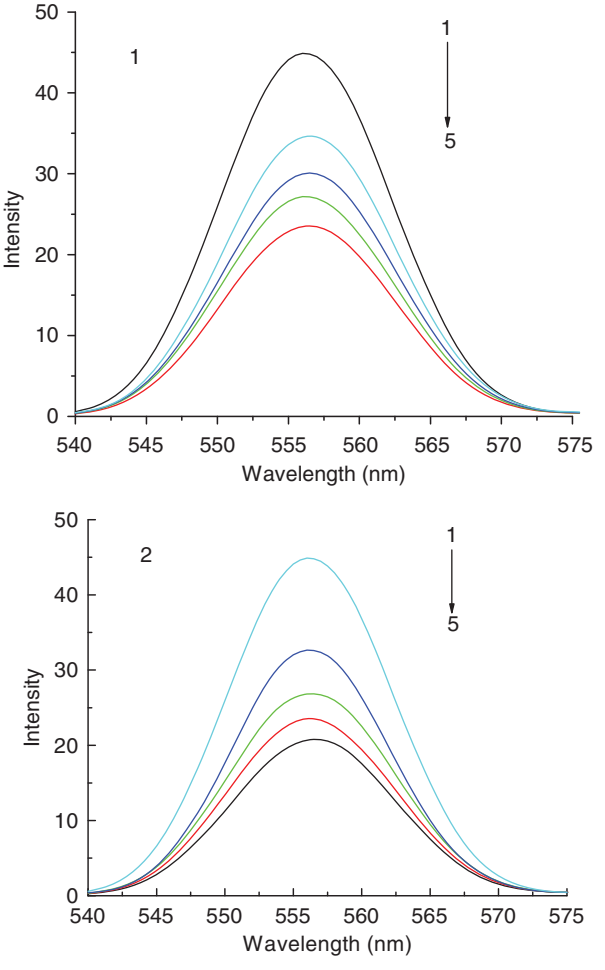

Figure 4. Emission spectrum of EB bound to DNA in the presence of **1** and **2**, ([EB] = 1 μmol L^{-1}, [DNA] = 2.5 μmol L^{-1}, [complex] = 0–17 μmol L^{-1}, λ_{ex} = 526 nm). The arrow shows the intensity changes on increasing complex concentration.

3.2. *Fluorescence spectroscopic properties*

Fluorescence quenching measurements can be used to monitor metal binding [34]. The molecular fluorophore EtBr emits intense fluorescence in the presence of HC-DNA due to its strong intercalation between adjacent DNA base pairs. It was previously reported that quenching of DNA-EtBr fluorescence by addition of complexes causes a reduction in the emission intensity, indicating competition between the complex and EtBr in binding to DNA [35]. The study involves addition of the complexes to DNA pretreated with EtBr ([DNA]/[EtBr] = 2.5) and measurement of the intensity of emission [36]. The emission spectra of EtBr bound to DNA in the absence and presence of the two complexes are shown in figure 4 [37–39]. Fluorescence intensity of DNA-EtBr complex gradually reduces with the addition of **1** or **2**. The more the DNA-EtBr complex added, the lower was its fluorescence intensity. It can also be seen from figure 4 that the

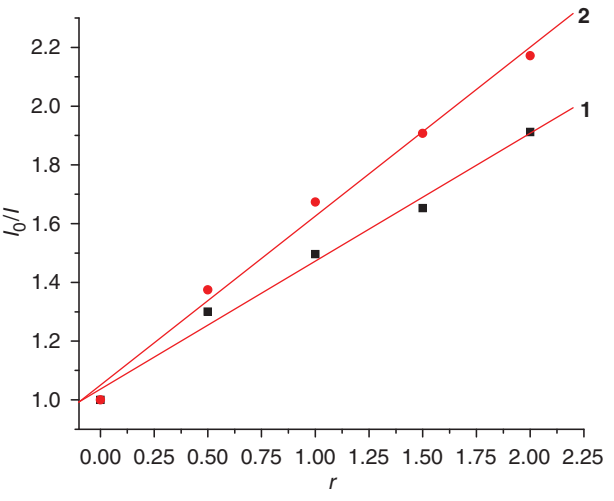

Figure 5. Stern–Volmer quenching plots of **1** and **2** with the value of slope 0.4352 for **1** and 0.5751 for **2**.

intercalation of the complexes into DNA is different with **2** being higher than that of **1** due to the presence of an extended aromatic planar ring.

Efficiencies of the two complexes binding to DNA are compared quantitatively, according to the classical Stern–Volmer equation: $I_0/I = 1 + K_{sq}r$, where I_0 and I represent the fluorescence intensity in the absence and presence of the complex, respectively, and r is the concentration ratio of the complex to DNA. K_{sq} is a linear Stern–Volmer quenching constant dependent on the ratio of the bound concentration of EtBr to the concentration of DNA [40]. The K_{sq} value is obtained as the slope of I_0/I *versus* r linear plot. The fluorescence-quenching curves of DNA-bound EtBr in the absence and presence of the two complexes are given in figure 5. The K_{sq} value of **2** is higher than that of **1**. The values of K_{sq} are 0.5751 and 0.4352, respectively. Accordingly, the intercalation ability of **2** into DNA is stronger than that of **1** [41].

3.3. *Gel electrophoresis study*

The influence of the complexes on the structure of DNA is evaluated by their DNA-cleavage ability [42–44], which can be monitored by agarose gel electrophoresis [45–47]. In the electrophoresis experiments, intact supercoiled DNA migrates fast (Form I), open circular DNA migrates slowly (Form II) and linear DNA occurs between Form I and II (Form III) [11]. The DNA used in the present studies is extracted from HeLa cells in our laboratory [48, 49]. The results of the electrophoresis experiments for the two complexes with HC-DNA are shown in figure 6. These complexes induce obvious cleavage of the HC-DNA at 13.2, 6.6 and 3.3 μmol L^{-1}; HC-DNA is cut into small molecular DNA. Lanes 2 and 5 show that supercoiled HC-DNA (Form I) gradually decreased about 70%, open circular form (Form II) gradually increased, and linear form (Form III) appeared. Capability of cleavage is stronger at high concentration than that at low concentration, which is consistent with the tendency in fluorescence quenching experiments.

To further illustrate cleaving efficiency of the two complexes, the experimental results of optical density scanning are shown in figure 7, obtained through optical density

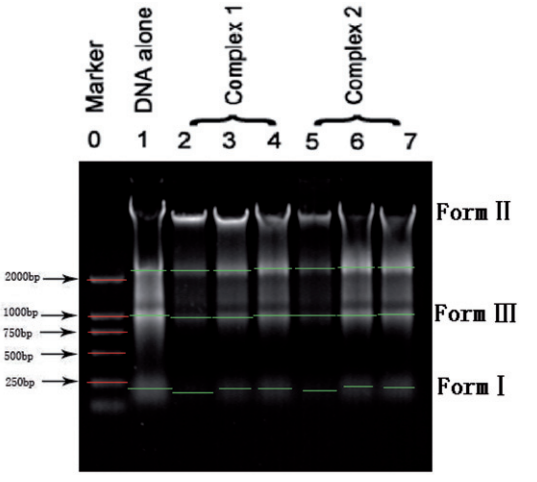

Figure 6. DNA strand break in HeLa cells treated with **1** and **2**. Lane 0: Marker; Lane 1: DNA alone; Lanes 2–7: different concentration of the complex: (2) 13.2; (3) 6.6; (4) 3.3; (5) 13.2; (6) 6.6; (7) 3.3 μm (lanes 2–4: **1**, lanes 5–7: **2**).

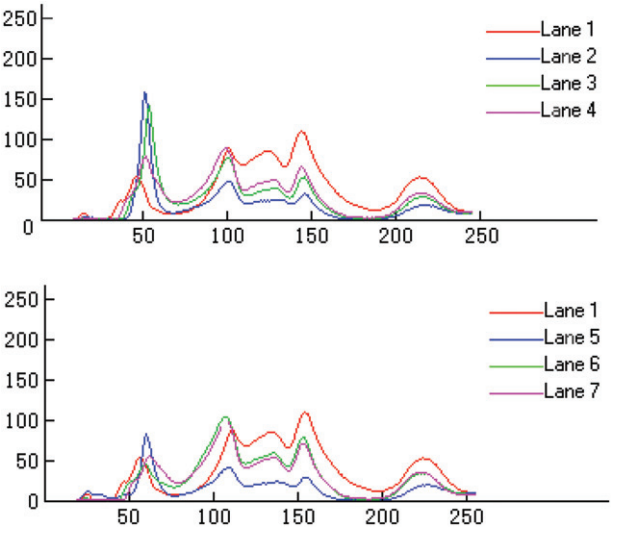

Figure 7. DNA-cleavage activity of **1** and **2** by the optical density scanning experiment.

scanning experiment of figure 6. Figure 7 shows the effect of HC-DNA cleavage varies in different concentrations. The peak value of lane decreases with gradual increase of concentration of complexes, showing the remainder of DNA base pair is sparse with increase of concentration of complexes. The two complexes in the present work exhibit strong cleaving ability for the HC-DNA.

3.4. *Cytotoxicity study*

The prepared complexes were tested for their cytotoxic activity *in vitro* by MTT assay. IC_{50} values were estimated for four human tumor cell lines, HeLa, Hep-G2, KB, and

Table 3. Cytotoxicity of the complexes against selected human tumor cells after 72 h of incubation.

Complex	IC_{50} $(\mu mol\,L^{-1})^{-1}$			
Tumor	HeLa	Hep-G2	KB	AGZY-83a
Complex **1**	9.45 ± 1.36	3.13 ± 0.91	4.53 ± 1.24	20.79 ± 4.21
Complex **2**	7.81 ± 1.11	2.81 ± 0.69	3.68 ± 1.03	16.53 ± 3.74
Cisplatin	0.79 ± 0.21	1.73 ± 0.47	1.42 ± 0.29	2.05 ± 0.49

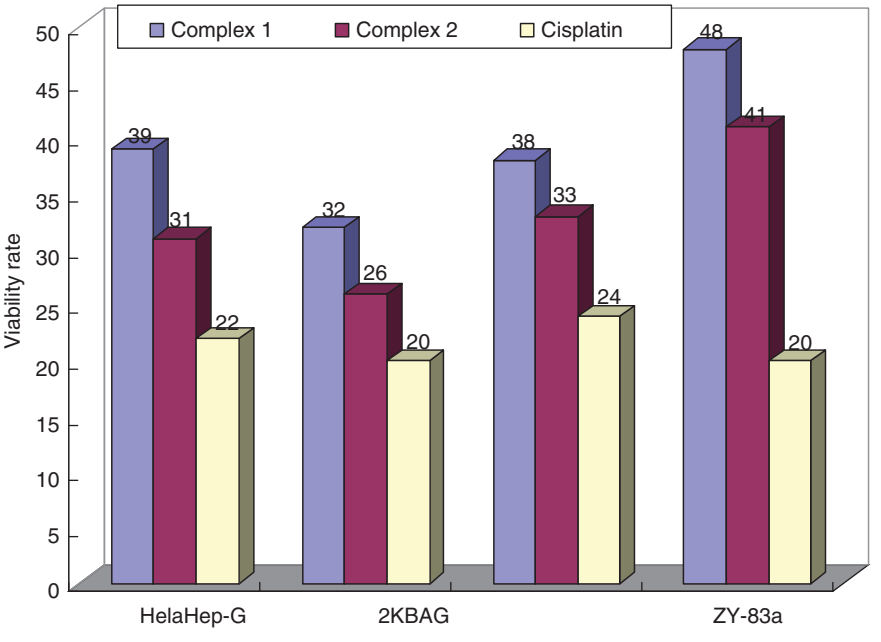

Figure 8. Effect of $3.0\,mg\,mL^{-1}$ of the complexes on breast cancer cells viability after 72 h of incubation. All determinations are expressed as percentage of the control (untreated cells).

AGZY-83a, summarized in table 3. The complexes both have certain anti-tumor activities which are inferior to those of cisplatin. The activity of **2** is stronger than that of **1** and the activity of the two complexes on Hep-G2 cells is stronger than on other cells. Figure 8 reveals the effect on cell growth after a treatment period of 72 h at $3.0\,mg\,mL^{-1}$ concentration. A viability rate less than 50% of the control values (untreated cells) is observed for treatment of complexes. The viability rate for the treatment of **2** is smaller than that of **1**, which coincides with the IC_{50} values.

3.5. In vitro *apoptotic study*

Cell apoptosis is the process of programmed cell death. When the cells are treated with the complexes, cell apoptosis may occur. The changes of size and morphology of the cells can be observed by dying them with hematoxylin-eosin. The normal intact HeLa

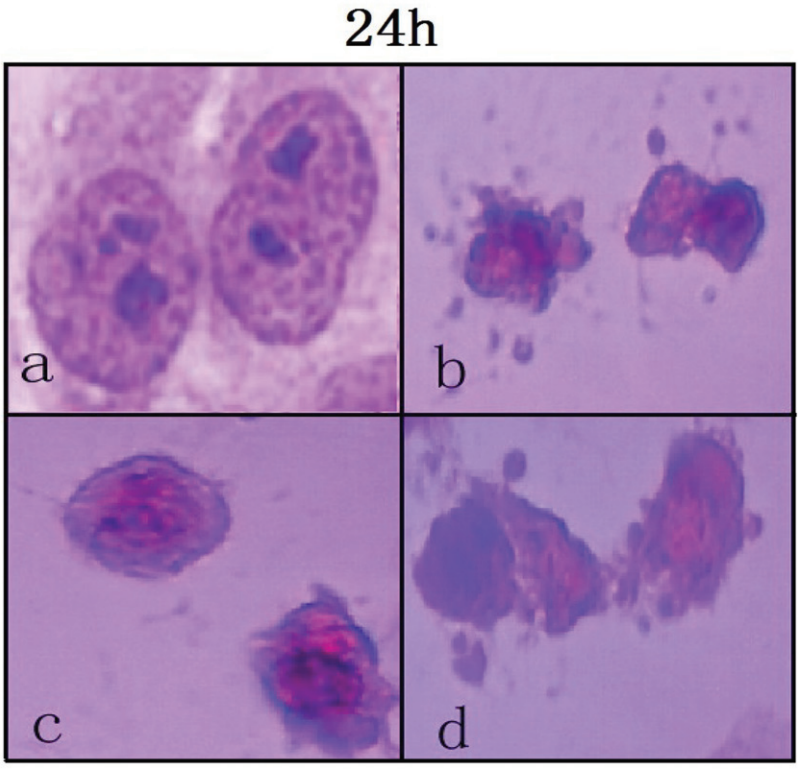

Figure 9. Morphological changes of HeLa cells. (a) normal HeLa cells for 24 h; (b) HeLa cells treated with cisplatin for 24 h; (c) HeLa cells treated with **1** for 24 h; (d) HeLa cells treated with **2** for 24 h.

cells exhibit dense state and intercellular tight junction; single cell is polygonal in shape or irregular cell morphology and cytoplasm is a clear appearance (shown in figure 9a). Figure 9(b), (c), and (d) are HeLa cells treated with cisplatin, **1** and **2** for 24 h. These figures are different from figure 9(a), where the cell nucleus became pyknotic (shrunken and dark) and condensed chromatin located on the nuclear membrane. As stated previously, the two complexes have apoptosis on the HeLa cells, but lower than cisplatin. In the present work, morphological changes of the HeLa cells have been observed under the optical microscope.

4. Conclusions

A carboxylic acid ligand (dibe = 2,2-dibenzylmalonate acid) was synthesized. We report synthesis and characterization of two complexes, $[Mn(L^1)_2(dibe)_2](L^1)$ (**1**) and $[Mn(L^2)_2(dibe)_2]$ (**2**). The DNA-binding properties of the complexes were examined by fluorescence spectra, which suggested their involvement in intercalative DNA interaction with different binding affinities. The cleavage of HC-DNA by the complexes was investigated using agarose gel electrophoresis, and the results indicate that the

complexes exhibit efficient DNA cleavage. Cytotoxic studies show that the two complexes exhibit cytotoxic activity against different cell lines tested in general and are especially effective against Hep-G2 cell lines. Additionally, the apoptotic tests indicate that the complexes had an apoptotic effect on HeLa cells.

Acknowledgements

We gratefully acknowledge the Natural Science Foundation of China (No. 20971090, 21171118), the science and technology projects fund of Shenyang City (No. F10-215-1-00).

References

[1] E.J. Gao, L. Liu, M.C. Zhu, Y. Huang, F. Guan, X.N. Gao, M. Zhang, L. Wang, W.Z. Zhang, Y.G. Sun. *Inorg. Chem.*, **50**, 4732 (2011).
[2] J. Bogojeski, Z.D. Bugarcic, R. Puchta, R. van Eldik. *Eur. J. Inorg. Chem.*, 5439 (2010).
[3] I.A. Danish, C.S. Lim, Y.S. Tian, J.H. Han, M.Y. Kang, B.R. Cho. *Chem. Asian J.*, **6**, 1234 (2011).
[4] W.J. Tan, J. Zhou, F.Y. Li, T. Yi, H. Tian. *Chem. Asian J.*, **6**, 1263 (2011).
[5] J.S. Kim, W.J. Rieter, K.M.L. Taylor, H. An, W. Lin, W. Lin. *J. Am. Chem. Soc.*, **129**, 8962 (2007).
[6] S. Komeda, M. Lutz, A.L. Spek, M. Chikuma. *Inorg. Chem.*, **39**, 4230 (2000).
[7] J. Ruiz, J. Lorenzo, C. Vicente, G. Lopez, J.M. Lopez-de-Luzuriaga, M. Monge, F.X. Aviles, D. Bautista, V. Moreno, A. Laguna. *Inorg. Chem.*, **47**, 6990 (2008).
[8] A.M. Angeles-Boza, P.M. Bradley, P.K.-L. Fu, S.E. Wicke, J. Bacsa, K.R. Dunbar, C. Turro. *Inorg. Chem.*, **43**, 8510 (2004).
[9] A. Bakalova, H. Varbanov, R. Buyukliev, G. Momekov, D. Ferdinandov, S. Konstantinov, D. Ivanov. *Eur. J. Med. Chem.*, **43**, 958 (2008).
[10] T. Tanaka, K. Yukawa, N. Umesaki. *Oncol. Rep.*, **14**, 1365 (2005).
[11] V. Rajendiran, R. Karthik, M. Palaniandavar, H. Stoeckli-Evans, V.S. Periasamy, M.A. Akbarsha, B.S. Srinag, H. Krishnamurthy. *Inorg. Chem.*, **46**, 8208 (2007).
[12] S. Ramakrishnan, V. Rajendiran, M. Palaniandavar, V.S. Periasamy, B.S. Srinag, H. Krishnamurthy, M.A. Akbarsha. *Inorg. Chem.*, **48**, 1309 (2009).
[13] S. Rani-Beeram, K. Meyer, A. McCrate, Y. Hong, M. Nielsen, S. Swavey. *Inorg. Chem.*, **47**, 11278 (2008).
[14] V. Onnis, M.T. Cocco, V. Lilliu, C. Congiu. *Bioorg. Med. Chem.*, **16**, 2367 (2008).
[15] M. Yodoshi, N. Okbe. *Chem. Pharm. Bull.*, **56**, 908 (2008).
[16] B. Selvakumar, V. Rajendiran, P.U. Maheswari. *J. Inorg. Biochem.*, **100**, 316 (2006).
[17] E.J. Gao, M.C. Zhu, L. Liu, Y. Huang, L. Wang, C.Y. Shi, W.Z. Zhang, Y.G. Sun. *Inorg. Chem.*, **49**, 3261 (2010).
[18] E.J. Gao, L. Wang, M.C. Zhu, L. Liu, W.Z. Zhang. *Eur. J. Med. Chem.*, **45**, 311 (2010).
[19] E.J. Gao, K.H. Wang, M.C. Zhu, L. Liu. *Eur. J. Med. Chem.*, **45**, 2784 (2010).
[20] E.J. Gao, Q. Wu, C.S. Wang, M.C. Zhu, L. Wang, H.Y. Liu, Y. Huang, Y.G. Sun. *J. Coord. Chem.*, **62**, 3425 (2009).
[21] E.J. Gao, M.C. Zhu, H.X. Yin, L. Liu, Q. Wu, Y.G. Sun. *J. Inorg. Biochem.*, **102**, 1958 (2008).
[22] E.J. Gao, M.C. Zhu, Y. Huang, L. Liu, H.Y. Liu, F.C. Liu, S. Ma, C.Y. Shi. *Eur. J. Med. Chem.*, **45**, 1034 (2010).
[23] E.J. Gao, T.D. Sun, S.H. Liu, S. Ma, Z. Wen, Y. Wang, M.C. Zhu, L. Wang, X.N. Gao, F. Guan, M.J. Guo, F.C. Liu. *Eur. J. Med. Chem.*, **45**, 4531 (2010).
[24] E.J. Gao, L. Lin, Y. Zhang, R.S. Wang, M.C. Zhu, S.H. Liu, T.D. Sun, W. Jiao, V.Z. Andrey. *Eur. J. Med. Chem.*, **46**, 2546 (2011).
[25] E.J. Gao, X.N. Gao, F. Guan, M.C. Zhu, L. Liu, M. Zhang, Y.X. Zhang, Y. Wang, Z. Wen, Y. Zhang, Y. Zhang, Q. Liang. *Eur. J. Med. Chem.*, **46**, 160 (2011).
[26] J.F. Song, R.S. Zhou, T.P. Hu, Z. Chen, B.B. Wang. *J. Coord. Chem.*, **63**, 4201 (2010).
[27] C.Y. Sun, S. Gao, L.P. Jin. *Eur. J. Inorg. Chem.*, 2411 (2006).
[28] Y.G. Sun, X.F. Gu, E.J. Gao, S.D. Chen. *Chin. J. Struct. Chem.*, **25**, 1431 (2006).

[29] T. Chatterjee, M. Sarma, S.K. Das. *Cryst. Growth Des.*, **10**, 3149 (2010).
[30] R.S. Kumar, S. Arunachalam, V.S. Periasamy, C.P. Preethy, A. Riyasdeen, M.A. Akbarsha. *Eur. J. Med. Chem.*, **43**, 2082 (2008).
[31] D. Quinonero, P.M. Deya, M.P. Carranza, A.M. Rodrıguez, F.A. Jalon, B.R. Manzano. *Dalton Trans.*, **39**, 794 (2010).
[32] E.J. Gao, L. Liu, M.C. Zhu, Q. Wu. *Chin. J. Chem.*, **27**, 1285 (2009).
[33] V. Chandrasekhar, K. Gopal, S. Nagendran, A. Steiner, S. Zacchini. *Cryst. Growth Des.*, **6**, 267 (2006).
[34] W.J. Mei, J. Liu, H. Chao, L.N. Ji, A.X. Li, J.Z. Liu. *Transition Met. Chem.*, **28**, 852 (2003).
[35] E.J. Gao, Y.G. Sun, Q.T. Liu, L. Duan. *J. Coord. Chem.*, **59**, 1295 (2006).
[36] M.T. Cocco, C. Congiu, V. Lilliu, V. Onnis. *Bioorg. Med. Chem.*, **15**, 1859 (2007).
[37] G.Y. Bai, K.Z. Wang, Z.M. Duan, L.H. Gao. *J. Inorg. Biochem.*, **98**, 1017 (2004).
[38] S. Wirth, C.J. Rohbogner, M. Cieslak, J. Kazmierczak-Baranska, S. Donevski, B. Nawrot, I.P. Lorenz. *J. Biol. Inorg. Chem.*, **15**, 429 (2010).
[39] B.C. Baguley, M. Le Bret. *Biochemistry*, **23**, 937 (1984).
[40] J.R. Lakowicz, G. Weber. *Biochemistry*, **12**, 4161 (1973).
[41] S. Ghosh, A.C. Barve, A.A. Kumbhar, A.S. Kumbhar, V.G. Puranik, P.A. Datar, U.B. Sonawane, R.R. Joshi. *J. Inorg. Biochem.*, **100**, 331 (2006).
[42] Q.X. Xiang, J. Zhang, P.Y. Liu, C.Q. Xia, Z.Y. Zhou, R.G. Xie, X.Q. Yu. *J. Inorg. Biochem.*, **99**, 1661 (2005).
[43] J. Qian, W. Gu, H. Liu, F.X. Gao, L. Feng, S. Yan, D.Z. Liao, P. Cheng. *Dalton Trans.*, 1060 (2007).
[44] B. Macías, M.V. Villa, B. Gómez, J. Borrás, G. Alzuet, M. González-Álvarez, A. Castiñeiras. *J. Inorg. Biochem.*, **101**, 444 (2007).
[45] J.L. García-Giménez, M. González-Álvarez, M. Liu-González, B. Macías, J. Borrás, G. Alzuet. *J. Inorg. Biochem.*, **103**, 923 (2009).
[46] C.Y. Shi, E.J. Gao, S. Ma, M.L. Wang, Q.T. Liu. *Bioorg. Med. Chem. Lett.*, **20**, 7250 (2010).
[47] T. Ohse, S. Nagaoka, Y. Arakawa, H. Kawakami, K. Nakamura. *J. Inorg. Biochem.*, **85**, 201 (2001).
[48] R.G.M. Moreno, M.V. Alipazaga, O.F. Gomes, E. Linares, M.H.G. Medeiros, N. Coichev. *J. Inorg. Biochem.*, **101**, 866 (2007).
[49] S. Dhar, M. Nethaji, A.R. Chakravarty. *Inorg. Chem.*, **44**, 8876 (2005).